This is a manuscript submitted to the journal for publication consideration. The published version can be obtained directly through the publisher. This should be cited as follows:
Corkum AG, Martin CD (2004) Analysis of a rock slide stabilized with a toe-berm: A case study in British Columbia, Canada. International Journal of Rock Mechanics and Mining Sciences 41:1109–1121. https://doi.org/10.1016/j.ijrmms.2004.04.008

Analysis of a rock slide stabilized with a toe-berm

A. G. Corkum[a] *, C. D. Martin[a]
[a]Dept. Civil & Environmental Engineering, University of Alberta, Edmonton, Alberta, Canada

Submitted 2003 October 30

Abstract
Practical experience has shown that slope movements can be controlled by the placement of berms near the toe of the moving mass. During construction of the Revelstoke project, excavation of a large highway rock cut triggered movement of a 250,000 m^3 rock slide. A 15,000 m^3 toe-berm was used as a temporary measure to control the displacements of the slide and allow permanent remedial measures to be completed. The rock slide was extensively investigated and monitored. Because there is no direct linkage between factor of safety and deformations, limit equilibrium methods have not proven to be particularly effective when evaluating slope displacements. Therefore the three-dimensional distinct element program, *3DEC*, which is well suited for modelling rock masses, was used to investigate the stabilizing effect of the toe-berm on the slope deformations. In addition, *3DEC* was used to investigate the effect of internal discontinuities on slope displacements.

Keywords: Distinct element analysis, numerical modelling, slope stabilization, toe-berm.

1. Introduction

Limit equilibrium analyses, such as the method of slices, are routinely used to design rock slopes. These methods assess stability based on statics with no provision for directly linking stability with displacements. However, provided the factor of safety remains significantly above 1, displacements within the slope are adequately controlled and the slope behaviour is approximately elastic. Hence when movement is detected in a slope, limit equilibrium methods are not suitable for evaluating the impact of such movements on the overall stability [1]. Practical experience has shown that toe-berms can be effective in stabilizing moving slopes. The notion behind the use of toe berms is to provide sufficient dead weight or restraint near the toe of the unstable mass to control slope movement [2]. For example Arnao et al. [3] described the use of a 480,000 m^3 buttress to stabilized a 260 m high slide up to 50-m-thick in the abutment of the Tablachaca Dam; **?**] discussed the use of 0.7 M m^3 toe-berm to stabilize the 4.3 million m^3 Jackson Creek landslide, in New Zealand; and Fell et al. [4] describe the use of a toe-berm to stabilized the Hue Hue Road landslide in New South Whales, Australia.

During the construction of the Revelstoke project between 1977 and 1983, excavation of a large highway cut triggered movement of a 250,000 m^3 rock mass. The sliding mass, referred to as the 731 Block (Fig. 1), was extensively monitored and a temporary 15,000 m^3 toe-berm of rock fill placed against the northern half of the slope face stabilized the block until permanent remedial measures were successfully completed. While the toe-berm proved to be an effective slope stabilizer for the 731 Block, it is not clear why such a small rock volume, in comparison to the slide volume, was effective in controlling the slope movements. This paper describes a series of analyses that were carried out to investigate the interaction of slope displacements and the stabilizing toe-berm. The analyses were conducted using both two dimensional limit equilibrium and three dimensional distinct element methods.

Fig. 1: Photo of the 731 Block shortly after remedial measures were completed in 1980. Photo courtesy of B.C. Hydro.

*Corresponding author.
Tel: +1 (780) 492-3346, Email: acorkum@ualberta.ca

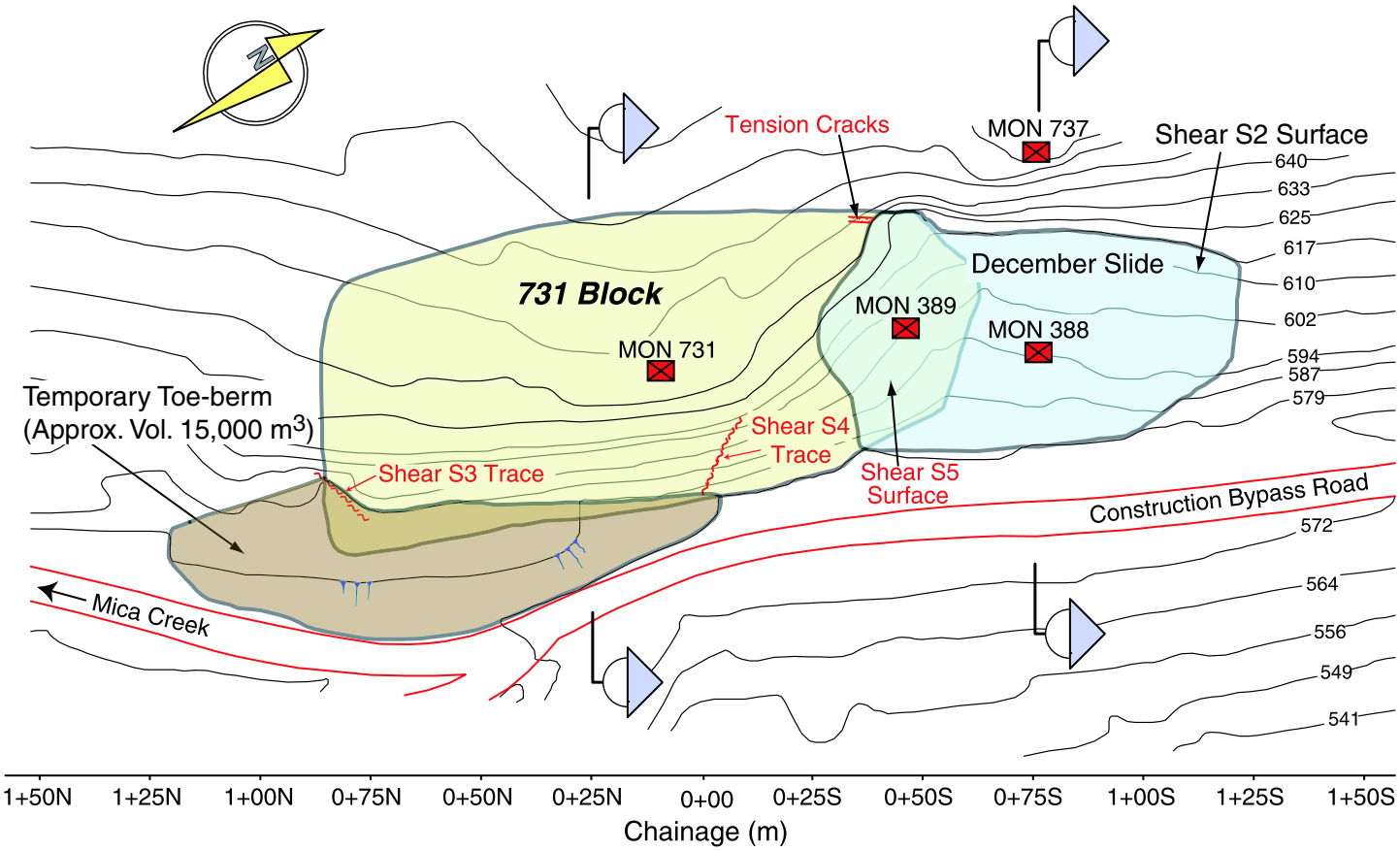

(*a*) Plan view

(*b*) Photo of the study area

Fig. 2: Location plan and photograph of the December Slide, the 731 Block and the toe-berm used to control the 731 Block movements.

2. Background

The Revelstoke Dam was completed in 1983 at a location approximately 5 km upstream of the town of Revelstoke, in the Selkirk mountains of British Columbia. The project consisted of the construction of a 160 m high concrete gravity dam and a 1.2 km long, 70 m high earthfill dam and rock cuts for the relocation of a bypass highway. The geological setting for the project is given by Lane [5] and can be summarized as a sequence of metasediments that dipped from West to East.

The rock excavations for the project presented ample engineering challenges due to unfavorable geological conditions [6]. One notable rock engineering challenge was excavation of the Highway 23 bypass road cuts. The excavations for this highway relocation paralleled the left (East) bank of the river valley. On this side of the valley the foliation of the metasediments generally strikes parallel to the river valley and dips less than 15° towards the East, into the rock cuts.

2.1. December Slide

The rock excavations for the highway relocation proceeded without incident until reaching an elevation about 10 to 15 m above final grade elevation. In early December 1978, a production blast triggered movement of about 30,000 m^3 of rock, known as the December Slide (Fig. 2). The uphill extent of the slide was bounded by an infilled near vertical fracture, the formation of which may be related to stress relief during valley formation. The vertical extent of the slide was bounded by a clearly identified shear zone referred to as *S2* (Fig. 3). No attempt was made to stabilize this slide and eventually the slide mass was completely removed and the geometry and condition of the slide base exposed. Gouge samples taken from *S2* contained approximately 55 percent fines (silt and clay) and hydrometer analysis indicated approximately 40 percent of this fine material was clay sized.

Monitoring of the slope was carried out using traditional survey techniques. Monument 388 was located in the middle of the slide while Monument 389 was located at the northern limit of the slide and Monument 737 was located above the slide, i.e., on the stable side of the infilled vertical fracture. Total horizontal movement recorded by Monument 388 was approximately 1000 mm, while only 130 mm was recorded by Monument 389 and no movement was recorded by Monument 737 (Fig. 4). During the active movement period the average velocity was approximately 28 mm/day and prior to the triggering 'blast' (see Fig. 4) reached a maximum velocity of 45 mm/day, based on Monument 388. The large amount of horizontal displacement resulted in the formation of a significant number of tension cracks in the sliding mass, particularly above elevation 610 m (Fig. 3). In essence the moving mass became a series of blocks sliding on an upper surfce of approximately 44 degrees. Movement of the slide eventually slowed after all construction activity near the toe of the slide was stopped. The deformed slope with somewhat flatter toe geometry, in conjunction with the work stoppage, is thought to have contributed to the reduction in velocity to approximately 1.2 mm/day. Drain holes were installed as part of the excavation design and some of the drain holes did initially produce water. However at the time of the slide the slope was considered dry, and groundwater was not a factor in the slope stability.

Intact hard rocks usually reach failure in laboratory testing at strains of less then 1 percent. The horizontal strain between Monuments 388 and 737 (differentiating the displacement field over horizontal distance) reached a maxi-

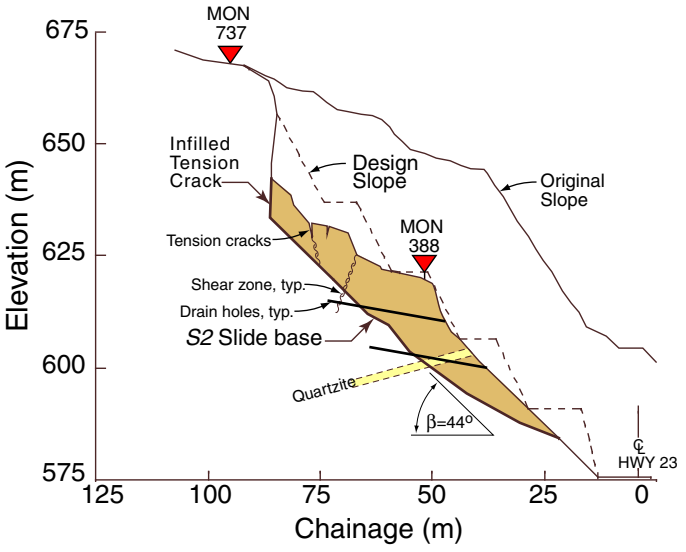

Fig. 3: Section of the December Slide. The movement was triggered by blasting near the toe of the slope and the slide base was determined after excavating the slide rock mass. See Fig. 2*a* for location.

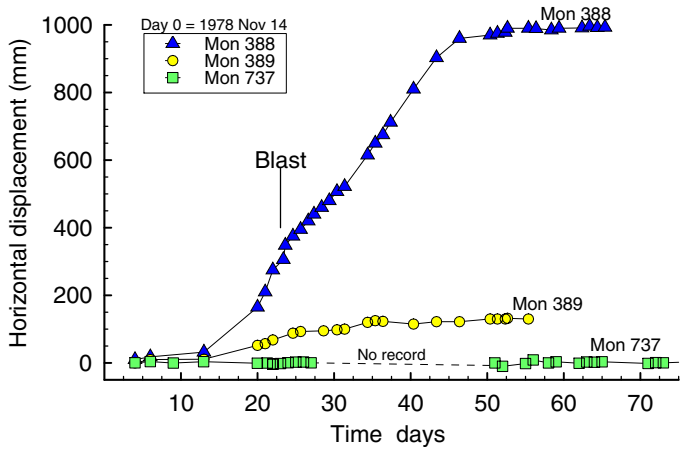

Fig. 4: Horizontal movement at Monuments 388 and 389 located on the December Slide and Monument 737 located off the slide. See Fig. 2*a* for monument locations.

mum of approximately 3.5 percent by the time the movements stopped. Approximately 300 mm of horizontal displacement would produce a strain of 1 percent over the distance considered. Whether this amount of displacement was sufficient to declare the slope had 'failed' can only be judiciously speculated on. Certainly with this displacement the upper part of the slide had started to break into blocks, as indicated by the formation of tension cracks. Interestingly, using an extensively instrumented highwall slope in Upper Cretaceous soft sandstones and mudstones at Highvale mine, Small and Morgenstern [7] concluded that failure of the slope occurred when local horizontal strains reached a maximum of 1 percent. For the slope in question at the Highvale mine, movement rates ranged from 1-3 mm/day for a duration of 50-70 days.

2.2. 731 Block

After the December Slide, monitoring of the rock slopes associated with the highway reallocation revealed that significant movement was occurring in the rock mass located immediately upstream of the December Slide. An oblique photograph of this block, known as the 731 Block, and the toe-berm used to stabilize the 731 Block is shown in Fig. 2.

The 731 Block is comprised mostly of quartzite gneiss with lesser amounts of hornblende gneiss and mica gneiss. Small quantities of pegmatite, marble and quartzite are also present. Most of the rock within the 731 Block is considered to be of moderate quality with rock quality designation (*RQD*) averaging between 35 and 55 percent [6]. The rock is generally of lower quality towards the north and south ends of the Block. The degree of weathering in drill core was described as mostly fresh stained to slightly weathered with more intense weathering occurring near original ground surface.

Four major shears were identified within the 731 Block (Fig. 5). The most significant feature with regard to stability of the 731 Block are the *S1* and *S2* shears. Shear *S1*, strikes 030 degrees and dips about 60 degrees east. Approximately 150 to 300 mm of soft gouge was observed along *S1* in the vicinity of the December Slide. In the 731 Block, this shear is a subvertical discontinuity in the mid-block region. A cross section through this rock mass is given in Fig. 5.

Shear *S2* dips out of the slope at about 35 degrees and forms the base of the December Slide and the interpreted base/slide surface of the 731 Block. Where it is exposed at the December Slide, Shear *S2* is an undulating zone containing 0.3 to 2 m of crushed rock with some clay gouge. The actual location where the slide surface daylights in the slope face was not well defined possibly because the slide was stabilized before an easily identifiable rupture surface was fully developed. Of less significance are shears *S3* and *S4*, both dipping about 45 degrees out of the slope. Shear *S5* forms the downstream face of the 731 Block (see Fig. 2).

The 731 Block was extensively instrumented and closely monitored during the investigation and construction stages. Eight boreholes were cored within the immediate vicinity of the 731 Block and the December Slide with nested piezometers installed in five of these holes for groundwater monitoring purposes. Additionally, a total of 6 surface survey monuments, 12 inclinometers and 7 nests of extensometers were installed for deformation monitoring. Although the surface monuments provided the longest record of deformation, they were the least accurate method and were difficult to correlate to specific movement zones within the rock mass (Fig. 6).

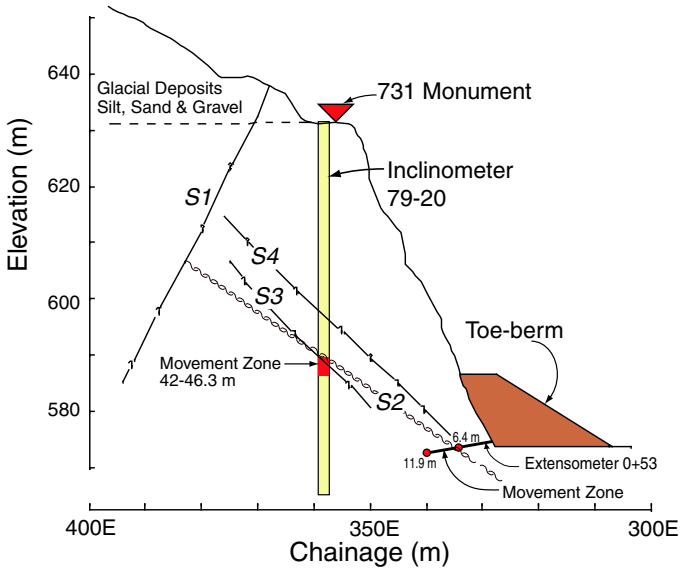

Fig. 5: Section through the 731 Block at Station 0+23 (m) North. See Fig. 2*a* for location.

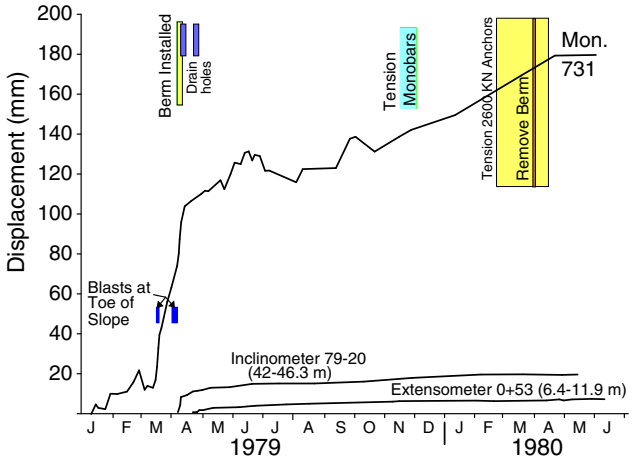

Fig. 6: Movement record for the 731 Block. It should be noted that Monument 731 was located at the crest of the block while the inclinometer and extensometer record movement across the shear zone at the base of the slide.

Only minor creep movement, approximately 0.2 mm/day, was recorded during the early stages of excavation. However, as a result of blasting and excavation at the toe of the 731 Block, movement accelerated rapidly to 3.6 mm/day (Fig. 6). With construction of the 15,000 m^3 temporary toe-berm, movement slowed drastically to 0.2 mm/day until installation of the permanent anchor system stopped the movement. Various instruments recorded deformations ranging from 10 to 180 mm. It should be noted that only the surface survey monuments were in place prior to the large slope movement, hence the extensometers and inclinometers only record a portion of this movement. Consequently the amount of total movement and the velocities recorded by these instruments were considerably less than those recorded for the December Slide.

Based on the piezometric records at the time of construction, the groundwater pressure acting on the base of the 731 Block was minor, usually less than one meter, even during periods of rapid recharge.

Since the completion of the remedial measures in 1980, which included the installation of a permanent anchor and drainage system, no additional significant movements have been recorded by the instruments that monitor the 731 Block (A.S. Imrie, B.C. Hydro, pers. comm.)

From the displacement monitoring that was carried out for the 731 Block, there is little doubt that the 15,000 m^3 temporary toe-berm played a significantly role in reducing the velocity from 3.6 mm/day to 0.2 mm/day. However, it is not intuitive, how a stabilizing mass, that is only 6% of the moving mass, could have such a significant effect. In the following sections the effect of the toe-berm is explored using a limit equilibrium method and a three-dimensional distinct element numerical method.

3. Toe-berm effect: Limit equilibrium analysis

As experienced during the Revelstoke Project, rock slides often consist of relatively rigid blocks sliding along a basal failure surfaces with internal adjustment taking place along subvertical discontinuities (Fig. 7). Martin and Kaiser [8] showed that the Sarma limit equilibrium method [9] had clear advantages over the traditional method of slices when evaluating the factor of safety of rock slopes that demonstrate this mode of behaviour. The Sarma method is a rigorous method, satisfing both force and moment equations of equilibrium [10]. Sarma utilizes a critical acceleration factor K_c, so named because of the association with the horizontal load used for solving earthquake related problems. The factor K_c gives the horizontal load as a fraction of the total weight of the free body. When applied to the free body, the horizontal force brings the forces along the slip surface into equilibrium with the available strength mobilized along the slip surface. The factor of safety is then defined as the factor by which the available shear strength should be reduced so as to bring the slide mass into equilibrium with the mobilized shear force.

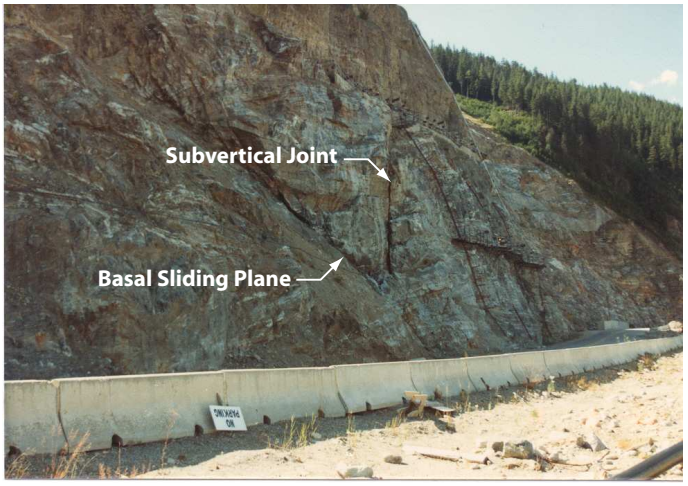

Fig. 7: Photo of the 731 Block looking south, showing the basal sliding plane and an example of a steeply dipping subvertical joint.

The Sarma method is particularly usefull for rock slope problems involving discrete discontinuities because it allows the user to specify the blocks/slices within the slide mass where movement may occur. In addition strength parameters differing from those of the basal slip surface my be assigned along the internal discontinuities. A computer program using Sarma's method, as modified by Hoek [11], was used to perform calculations discussed in this paper.

Because there was no laboratory testing performed on the materials that comprise the various shear zones associated with the Highway 23 rock cuts, the large-scale shear strength parameters were estimated by back analysis. The material comprising the December Slide was removed after failure, exposing the failure plane for surveying and more careful observation. This information, along with the slide geometry (Fig. 3), was used to back calculate the large-scale strength parameters that characterize the *S2* shear zone that formed the basal sliding plane of both the December Slide and the 731 Block.

For the December Slide, it is assumed that the large movements observed were sufficient to reduce the cohesion strength component to zero. Based on the work of Martin and Kaiser [8], the subvertical internal discontinuities used in the Sarma analysis, were assigned a friction angle of 40 degrees. Given the relatively shallow thickness of the December Slide and the free draining nature of the fractured rock mass, the piezometric pressures were considered to be negligible for all analyses.

Based on the back analysis of the December Slide, the large-scale mobilized angle of friction (ϕ) for the basal shear zone *S2* is estimated to be approximately 35 degrees with zero cohesion. These strength parameters provided a limiting equilibrium condition, i.e., factor of safety equal to unity. The 731 Block in Fig. 5 was then analyzed using the

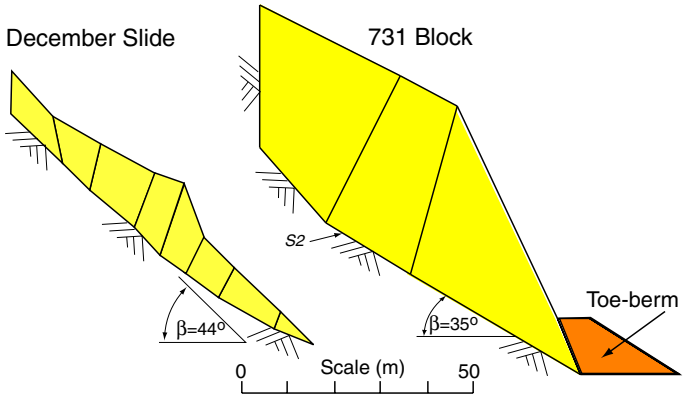

Fig. 8: Simplified sections of the December slide and 731 Block used in Sarma analyses.

Sarma Method and the strength parameters from the December Slide. This analysis also provided a Factor of Safety of approximately one. The simplified sections from these analyses are shown in Fig. 8.

The orientation of the base *(S2)* of the 731 Block in the vicinity of the toe-berm is unknown. Visual observations of the slide area and vicinity suggested it probably occurred in a similar orientation to that shown for the December slide (see Fig. 8). Factor of safety sensitivity analyses were carried out using the Sarma Method to evaluate the effect of a change in the slope angle near the toe of the slide on the stabilizing effects from the toe-berm. Fig. 9 presents the results from these analyses and shows that as the slope of *S2* decreases from 35° to 21° the factor of safety improves from less than 1% to 15%.

From these analyses, the effect of the toe-berm is estimated to improve the stability of the 731 Block between 1% and 15% for the various slide plane geometries. If the change in the *S2* slope angle is similar to that observed for the December Slide, it is likely that the improvement is closer to 15% than 1%. An improvement of 10 to 15% would intuitively be consistent with the observed reduction in movement rate of the 731 Block following placement of the toe-berm shown in Fig. 6. This difficulty with linking measured displacements with the calculated limit equilibrium factor of safety exemplifies one of the shortcomings of this approach and highlights that the absolute value of the factor of safety, in such situations, has little meaning. As demonstrated here, the long-term displacement monitoring is the the only practical means of evaluating the effectiveness of remedial measures, such as the toe-berm. In the next section a numerical method of analysis is used to assess the effect of the toe-berm on displacements.

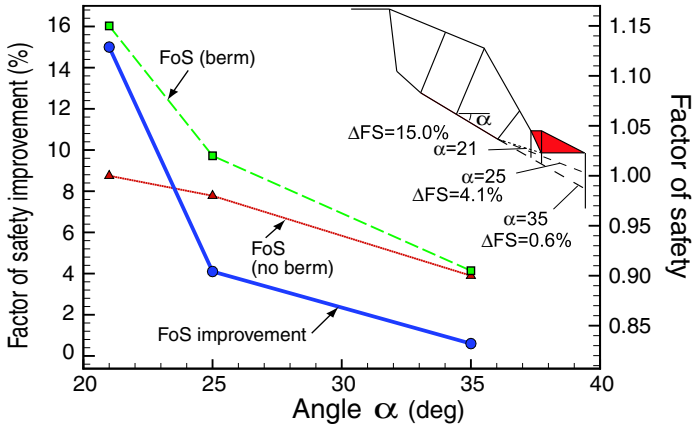

Fig. 9: Effect of the slope of failure surface *S2* in the vicinity of the toe-berm on the factor of safety.

4. Toe-berm effect: Distinct element analysis

Distinct element formulations are considered better suited for analyzing the post-failure behavior of a jointed rock mass than other methods such as finite element [1]. In this case, the distinct element code *3DEC*[1] was selected because of the need to observe movement of the 731 Block well into post-peak behavior. *3DEC* is a three-dimensional numerical code that utilizes a Lagrangian calculation scheme to model large movements and deformations of a blocky system. This allows for modelling of large movements and rotations, including complete detachment, of rigid or deformable discrete blocks [12]. The reaction of the model is calculated using the laws of motion advancing along a time marching scheme.

Although the 731 Block is relatively "data rich", as with most geotechnical problems it is considered "data limited" in terms of numerical modelling [13]. *3DEC* requires knowledge of the location of discontinuities within the rock mass. The simplified model geometry given in Fig. 10 was developed based on the geological model for the 731 Block and

[1]Available from Itasca Consulting Group, Inc. Minneapolis, USA

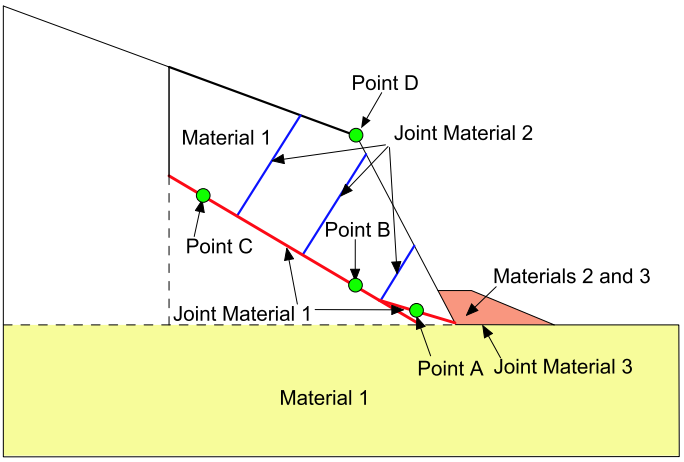

Fig. 10: Location of the various material models used in the *3DEC* model and the key observation points.

Table 1: Rock mass material properties used in the *3DEC* model.

Material No.	Density (kg/m^3)	K (MPa)	G (MPa)	ϕ (deg.)	Constit. Model
1	2800	19000	17000	–	Elastic Isotropic
2	2800	75	75	–	Elastic Isotropic
3	2600	75	75	40	Mohr-Coulomb Plasticity

the results from the limit equilibrium analysis. A bilinear shear surface along Shear S2, and daylighting in the vicinity of the toe of the excavation, was selected as the most likely failure surface geometry. The other critical geometrical simplifications/assumptions involve the frequency, location, and characteristics of internal block discontinuities.

4.1. Material properties and constitutive models

Because stress levels in the 731 Block are relatively low in comparison to the strength of intact rock, elastic deformation of intact rock was considered to be negligible in comparison to deformation along joints suggesting that a rigid block model would be appropriate. However, in order to accommodate excavation of the bench and placement of the toe-berm in *3DEC*, a more complex deformable block model was required. Therefore, an elastic, isotropic constitutive model was selected for the intact blocks of the slope while a Mohr-Coulomb plasticity model was used for the toe-berm material. This resulted in the three material models in Fig. 10: Material 1 represented the rock mass, Material 2 was the bench material at the toe of the slope prior to blasting and removal, and Material 3 represented the rock fill comprising the temporary toe-berm. The properties of these three materials is given in Table 1.

No testing had been carried out to determine the stiffness properties of the joints found in the 731 Block. The stiffness values reported by Infanti and Kanji [14] for joints at shallow depths were considered comparable for the 731 Block. Infanti and Kanji [14] reported that k_s values ranged from 0.02 GPa/m to 2 GPa/m over the normal stress range of 0.1 to 10 MPa. The 731 Block stresses are within the lower end of this range with the normal stress along the *S2* ranging from 0.1 to 3 MPa. Table 2 shows the dependence of joint stiffness parameters in relation to clay in-filling thickness. Although the discontinuities in the 731 Block contained variable amounts of clay gouge, the overall thickness of *S2* was substantially greater than those listed in Table 2. Therefore a range in stiffness values was evaluated.

The properties for the joints used to describe the 731 Block geometry given in Fig. 10 are given in Table 3. Joint Material 1 represents the basal Shear *S2* where the majority of deformation occurs while Joint Material 2 represents the near vertical internal discontinuities within the 731 Block. Joint Material 3 represents the contact surface between the toe-berm and the rock surface at the base of the slope.

The joint constitutive model provided in *3DEC* and used for all the joints in the 731 Block is referred to as the "joint area contact-Coulomb slip model". This model provides a linear representation of joint stiffness and yield limit and is based on: elastic stiffness, frictional, cohesive and tensile strength properties, and dilation characteristics common to rock joints. The model simulates displacement-weakening of the joint by loss of cohesive and tensile strength at the onset of shear or tensile failure.

4.2. Analysis procedure

The model geometry used to simulate the 731 Block is shown in Fig. 10. Tetrahedral zones were generated by *3DEC* for each block, and material and constitutive properties were assigned to the appropriate regions of the model (see Fig. 10). A zero displacement boundary condition was applied to the base and far-field sides of the model and gravity was activated. The model was then run for a sufficient number of time steps to reach equilibrium under gravity loading conditions. To prevent any slip or separation from occurring during initial gravity loading, high cohesion and tensile strength were temporarily applied to the joints while stepping to the initial state of force-equilibrium.

The rock slope in *3DEC* was excavated following the construction sequence used for the 731 Block. This resulted in a small bench at the toe of the slope, prior to the initiation of movement. At this point the model was again marched to equilibrium. This is the stage at which the model time was correlated to historical time just prior to blasting and removing the final bench initiating down slope movement of the 731 Block as shown in Fig. 6. Placement of the toe-berm

Table 2: Dependence of stiffness on clay-filling thickness, after Infanti and Kanji [14].

Clay-Filling Thickness (mm)	k_s (GPa/m)	k_n (GPa/m)	Ratio k_n/k_s
50 - 100	0.01 - 0.1	0.1 - 0.5	6
10 - 20	0.1 - 0.6	0.5 - 2.0	3.6
< 1	> 1.0	> 0.5	5

Table 3: Joint properties used in the *3DEC* model.

Joint	k_n (GPa/m)	k_s (GPa/m)	ϕ (deg.)	Constitutive Model
1	0.12	0.01	33	Coulomb Slip
2	0.12	0.01	40	Coulomb Slip
3	2.0	0.2	40	Coulomb Slip

in model time was based on comparison of model deformations with actual measured deformations. Finally the model was run for a sufficient number of time steps to observe the movement trend and effect of the toe-berm.

An important interpretive aid of *3DEC* modelling is the use of the History command. This command allows tracking of certain selected variables (e.g., displacements, stresses, strains) throughout the model during time stepping. This data was plotted as a means of evaluating model performance. A key variable that was tracked throughout is the unbalanced force within the model. This was a useful variable for interpreting a state of equilibrium. An unbalanced force decreasing to 1 or 0.1 percent of the maximum occurring in the model is considered a reasonable interpretation that equilibrium has been achieved [12].

4.3. Toe-berm Results

For soil slopes, Bishop [15] defined the factor of safety as the ratio of the actual soil shear strength to the minimum shear strength required to prevent failure. Because the factor of safety can be defined as a shear strength reduction factor, Dawson et al. [16] suggested that for numerical programs, such as *3DEC*, the factor of safety (F_ϕ) could be defined by:

$$F_\phi = \frac{\tan\phi}{\tan\phi_f} \tag{1}$$

where ϕ represents the actual friction angle of the material and ϕ_f is the friction angle that causes failure of the slope. By applying this strength-reduction approach to the strength parameters along the basal Shear *S2* the results from the limit equilibrium analysis can be compared to the factor of safety from the *3DEC* analysis.

The results of the strength reduction technique are shown in Fig. 11 and shows that ϕ is approximately 33 for a strength reduction factor of safety of unity. This is in reasonable agreement with the Limit equilibrium results which gave a factor of safety of unity for $\phi = 35°$. It should be noted that the shear surface in the *3DEC* model is planar, with no strength component due to roughness.

Since the shear stiffness of *S2* directly influences the slope deformations, a sensitivity analysis was carried out to assess the likely value of k_s. For these analyses k_n was held constant and ϕ was initially set at 35°. The resulting displacements for various values of k_s are given in Fig. 12. It is apparent from Fig. 12 that deformation increases rapidly for $k_s < 0.005$ GPa/m. It can also be seen in Fig 12 that k_s values in the range reported by Infanti and Kanji [14] resulted in deformations similar to those recorded from actual field measurements. For comparison, the model was also run with $\phi = 80°$ in order to evaluate the component of total deformation due to plastic yielding. The results indicate that a significant portion of displacement is due to elastic deformation.

The effect of elastic-plastic behaviour of *S2* can be seen by tracking the shear force versus shear displacement at Point B, in Fig. 10. For this analysis the following properties for the basal shear *S2* were used, based on the findings from the sensitivity analyses above: $k_s = 0.01$ GPa/m, $k_s = 0.12$ GPa/m, and $\phi = 33$ degrees. The results are given in Fig. 13 and show that the basal shear undergoes elastic deformation at a rate of about 0.4 MN/mm until 16 mm of deformation is reached. The beginning of plastic deformation is clearly defined in Fig. 13 and indicates, for these *S2* properties, the majority of slope movement can be attributed to plastic deformation.

As mentioned previously, *3DEC* time stepping occurs in an independent time frame. Therefore, movement in the *3DEC* model was matched to the actual recorded events of bench removal and construction of the toe-berm. This approximately synchronizes the *3DEC* model time to real increments of time. Using the base case properties for *S2*,

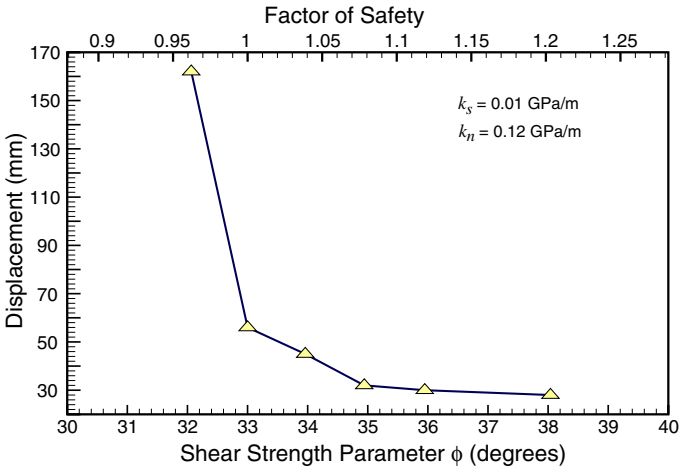

Fig. 11: Strength reduction method in 3DEC to determine the strength along shear S2.

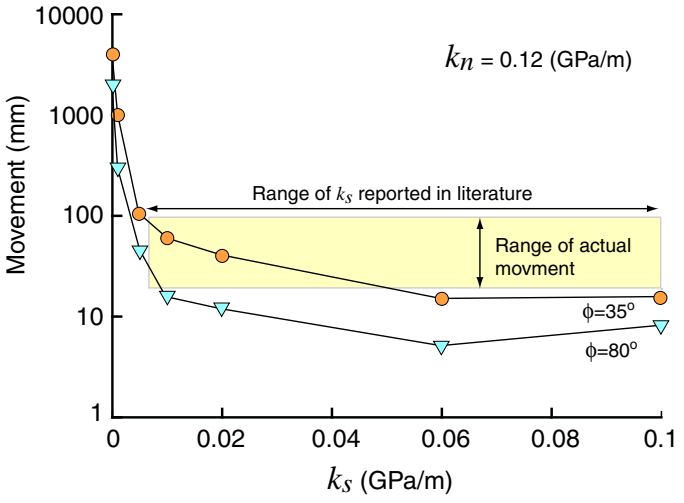

Fig. 12: Movement versus shear stiffness (k_s) with constant normal stiffness (k_n).

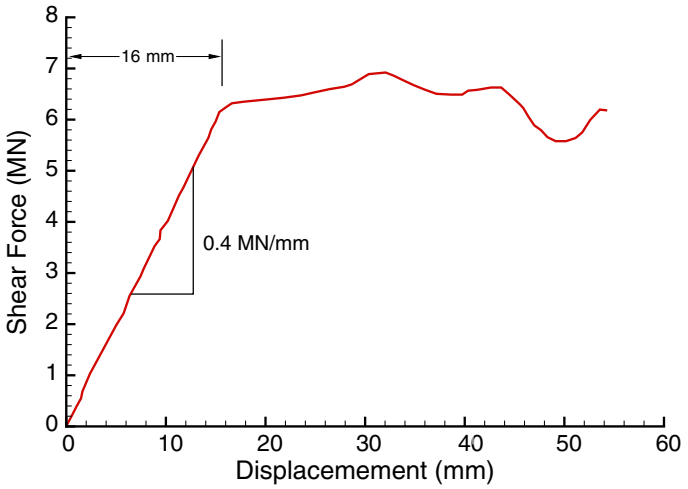

Fig. 13: Shear force versus shear displacement along shear *S2* (mid-block region), demonstrating the onset of plasticity along the failure surface.

the movement of the two key monitoring points were tracked in the *3DEC* model (Point D corresponding to the 731 Monument and Point A corresponding to Extensometer 0+23S, see Fig. 10). Fig. 14 shows the *3DEC* movement record for the two monitoring points compared to the actual movement. Cleary the deformation pattern generated by the model is not consistent with the measured deformations. In particular, the movement at the top of the slope (Point D) is less than that at the toe of the slope (Point A). This is in contrast to the measured displacement trends. It is perhaps unrealistic to expect the model displacements to match the measured displacements as the amount of model displacement is significantly dependent on the geometry and number of discrete blocks used to build the model and the dilation that occurs as the blocks displace. These issues will be explored further in the following section.

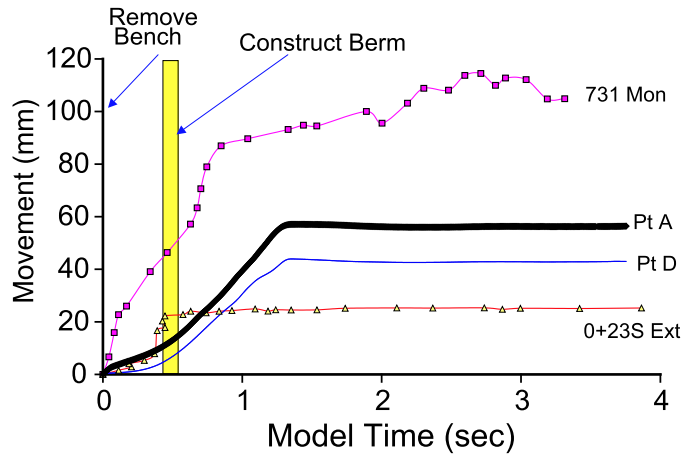

Fig. 14: Movement with time: Comparison of 3DEC model results with actual field measurements.

When the *3DEC* model was allowed to run without placing the toe-berm, the 731 Block appears to eventually reach a state of 'natural'. Fig. 15 shows that placement of the toe-berm reduced the total movement by approximately 20 mm at the toe, compared to not placing a berm. The results are similar for all locations tracked in the model. The equilibrium of the model being reached without the toe-berm is a consequence of the failure plane geometry at the toe of the slope. It implies that the geometry in the model does not permit the kinematic freedom necessary for the blocks to continue sliding. Whether the toe-berm provided that restraint in conjunction or independently of the slide toe geometry is unknown. Nonetheless Fig. 15 does show that even this small toe-berm was effective in reducing the total movements.

5. Inter-block joints and displacement patterns

As a rock slide mass moves down slope along an undulating, i.e., wavy, basal plane, it tends to 'break-up' as a result of localized stress concentrations and internal yielding, as observed in the December Slide. This results in an increased number of discontinuities or blocks, where internal shear displacement can occur. It is apparent that the simplified geometry and kinematic restrictions may have played a role in dominating the behavior of the *3DEC* model used to simulate the 731 Block. Therefore, additional *3DEC* modelling, based on the 731 Block slide, was used to explore the effects of internal kinematic restrictions on the overall deformation of the slide mass. This model is referred to as the "multi-block" model.

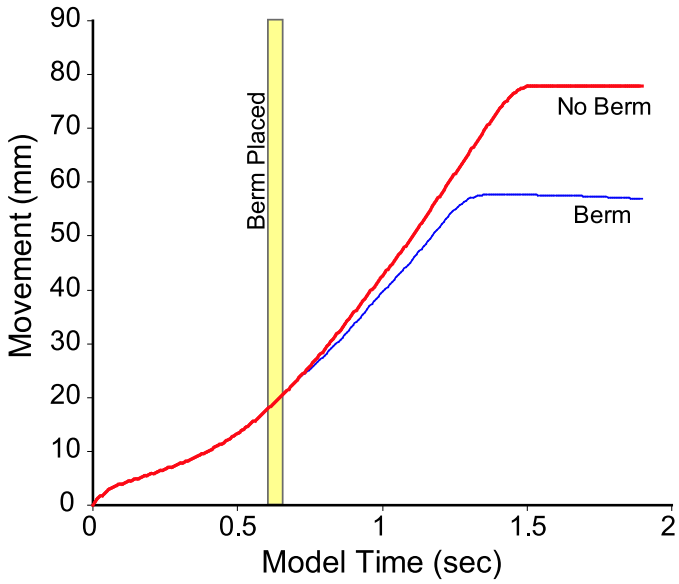

Fig. 15: Movement with time: with and without the berm.

5.1. Multi-block model

The general concept for the multi-block model was to observe the effect of increasing the number of inter-block discontinuities on the stability of a rock slope with a rough failure surface. The stability was evaluated in terms of deformations and a comparison was made with a planar failure surface. Both the undulating and planar failure surfaces are shown, as well as the toe-berm, in Fig. 16.

The *3DEC* multi-block model is about 200 m along the base, 150 m high and 100 m wide across the slope. A maximum of 8 inter-block discontinuities, with an average dip of about 55 degrees into the slope, subdivided the slide mass. Two cross-joints, dipping at an average of 40 degrees out of the slope, further divided the slide mass. To limit any 3-dimensional effects, the slope was divided through the middle with a vertical joint perpendicular to the slope face. In total the model consisted of 50 blocks, or 25 blocks in section (Fig. 16).

The *3DEC* multi-block model utilized two failure plane geometries for comparison purposes: (1) a planar failure surface dipping 30 degrees, and (2) a wavy failure surface consisting of two 'humps' and two 'troughs' that deviated from the average 30 degree plane by about 12 degrees. In order to prevent the slide mass from simply stopping at the bench below the slide mass, a 1 m drop off was provided between the bench below the slope and the location where the failure surface daylights. A rigid block model was used for the rock mass material with a density of 2500 kg/m^3. The *3DEC* Coulomb-slip constitutive model was used for all joints and the joint properties are given in Table 4.

The *3DEC* history functions were used to track the displacements along the basal failure surface at Points A, B and C (see Fig. 16. An additional function was created to calculate the dilation, or change in volume of the slide mass as it moved down slope. A total of 9 equally spaced points along the slope face were used to divide the slide mass into slices of average dimensions. This calculation did not include the backscarp development, only the change in volume within the slide mass itself. Tracking both the displacements along the failure surface and the overall volume change of the rock mass should provide further insights into the mechanisms of slope deformation.

Table 4: Joint properties used in the *3DEC* multi-block model.

Joint Type	k_n (GPa/m)	k_s (GPa/m)	ϕ (deg.)	c' (MPa)
Subvertical	0.12	0.01	28	0
Cross	0.12	0.01	45	1
Failure surface	0.12	0.01	30	0

5.2. Multi-block modelling results

In order to investigate the effect of internal discontinuities on slope behaviour, a series of *3DEC* models were carried out for 9 inter-block geometrical configurations with 2 cross-joints approximately parallel to the slide base and between 0 to 8 subvertical joints, corresponding to between 3 and 25 total blocks in section. All 9 of these models were performed for both 'wavy' and 'planar' failure surfaces, with and without the presence of a toe-berm, for a total of 36 model simulations. Fig. 17 shows the averaged displacement at points A, B and C for various multi-block models (number of blocks) on the undulating failure surface. From Fig. 17 it is clear that increasing the number of blocks resulted in larger displacements along the failure surface. In most cases the slide mass reached a point of stability/equilibrium prior to 15 seconds of model time (see Fig. 17). It should be noted that time is independent and cannot be used for direct com-

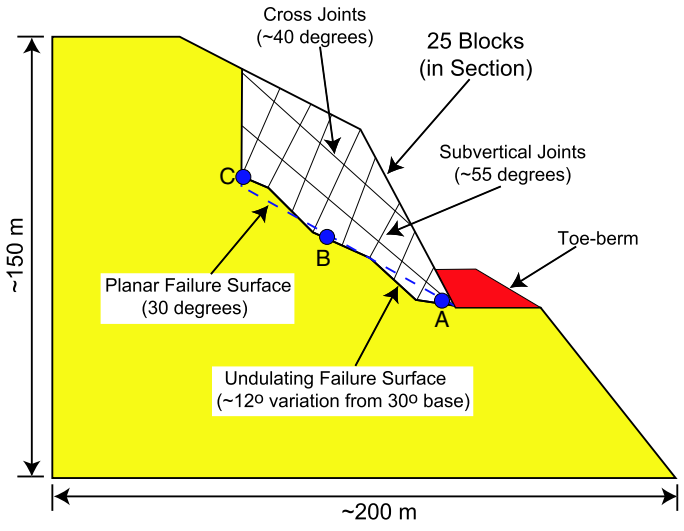

Fig. 16: The *3DEC* multi-block model geometry.

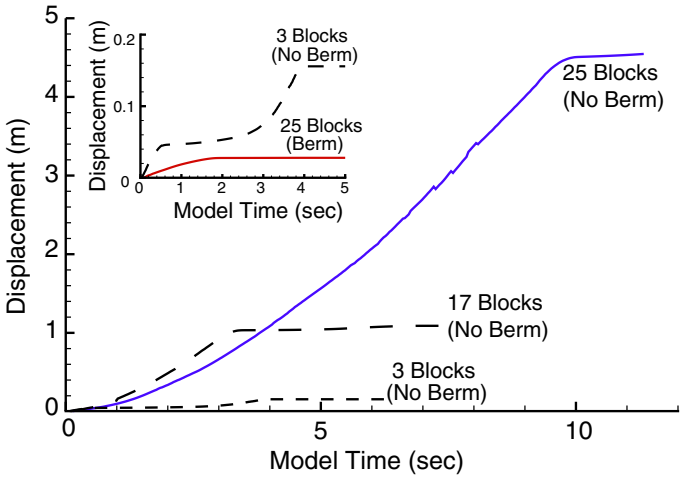

Fig. 17: Average slope displacement recorded at points A, B and C for various multi-block models using the undulating basal failure surface.

parison. The effect of the toe-berm is also shown in Fig. 17 for the 25 Block Model and clearly shows that the toe-berm decreased the total movement in the 25 Block Model.

Fig. 18 shows both the basal displacements and the volumetric dilation as a function of the number of blocks for both the planar and undulating failure surface without the toe-berm. For the planar failure surface the displacements were relatively constant and increased only slightly as the number of blocks increased. It was expected, for this case, that the number of internal blocks would have essentially no effect on basal plane displacements. However, the slightly sloping relation is likely due to the changes in kinematic freedom as the slide mass reached the bench located 1 m below the failure surface.

With the undulating failure surface, significant displacements (sliding) do not occur until the number of blocks is greater than 8. As the number of blocks increase from 10 to 25, the displacements and the volumetric dilation linearly increase. With only a few blocks on a wavy surface, kinematic freedom is not available to permit down-slope movement. The inset in Fig. 18 shows the displacement with increased number of blocks for the undulating failure surface with the presence of a toe-berm. In all cases analyzed, the toe-berm was very effective in reducing the amount of displacements, particularly for those cases where the number of blocks was greater than 8.

In a natural rock slope with a wavy failure plane, local yielding and breaking-up of the slide mass often occurs as down slope movement progresses (see the discussion on the December Slide). An attempt was made to simulate the effects of down slope movement combined with the rock slide breaking up into a larger number of blocks. Starting initially as a single block with the 2 cross joints in place, subvertical discontinuities were added as deformation increased. The subvertical joints were added starting near the toe and alternating between the toe and top of the slide mass, moving towards the middle. In this simulation, the subvertical joints were added at specified time intervals chosen to allow a contribution of each stage to the overall movement.

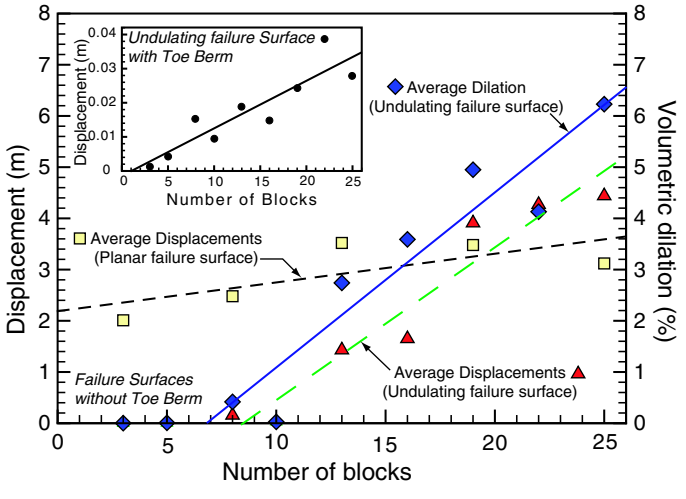

Fig. 18: Trends in the displacement and dilation patterns for slopes with different number of blocks without a toe-berm. The insert figure shows the effect of the toe-berm on the undulating failure surface.

Fig. 19 shows the trend of rapidly increasing displacement and volumetric dilation with down slope movement. Once the model contains more than 19 blocks, displacements rapidly accelerate. During the initial stages of sliding, the volumetric dilation tracks the failure surface displacements. This is not surprising because in this model all inter-block joints are planar, i.e, non-dilatant. However, with extremely large failure surface displacements, the rate of volumetric dilation accelerates suggesting large separation among the blocks. In a natural rock slope the roughness of the inter-block joints would likely cause this phenomena to occur at much smaller displacements along the basal failure-surface. In addition all the joints were modelled with a constant Coulomb-slip model, a strain-weakening slip model could also produce accelerating displacements at much smaller strains.

Because *3DEC* models a non-linear system as it evolves in time, the interpretation of results can be more subjective than with a conventional numerical program that produces a 'solution' at the end of its calculation phase. Nonetheless, for the results presented herein, every effort was made to interpret the results in a consistent and reproducible manner. In all the inter-block models, *3DEC* was cycled until trends were clearly defined. After about 8 blocks, deformations were dominated by plastic yielding. The final magnitudes of displacements were limited by the kinematics of the block-slope interaction. The trend of rapidly increasing deformations signifies the onset of collapse failure without a loss in strength along the sliding surface, as is commonly modelled. As indicated in Table 4 the stiffness properties assigned to all the joints were identical and represents very 'soft' joints. As a result the displacements reported here

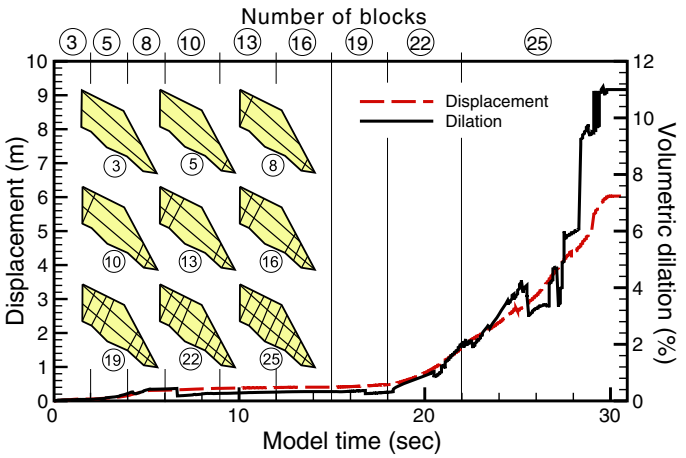

Fig. 19: Basal failure plane displacements and volumetric dilation as the sliding rock mass breaks-up into blocks.

for the inter-block models are much larger than might be anticipated in actual rock slopes.

In all the *3DEC* models with the undulating failure surface the effect of the toe-berm was to significantly reduce the displacements. By limiting the displacements, the ability of the rock mass to break-up into individual blocks reduces the risk of uncontrolled displacements leading to collapse failure. These findings are similar to those described by Martin and Kaiser [8] where rock bolt reinforcement was used to reduce the number of internal blocks and improve the overall stability of a large jointed rock slope.

6. Conclusions

A numerical model is intended to be an aid to thought rather than a substitute for thought (Starfield and Cundall 1988). The focus of this study was to use this approach to evaluate a field observation: a relatively small end-dumped rock-fill toe-berm was effective in controlling the displacements of a large moving rock mass. While this case study can be considered data-rich, considerable simplifications had to be made to apply the three-dimensional numerical model. Using reasonable parameters, based on geological interpretations, the numerical model responded in a manner that is logical and in general agreement with field observations.

Based on the Sarma limit equilibrium method, the toe-berm could have increased the stability of the slope by approximately 10 to 15% percent. Practical experience suggest that this magnitude of change in the factor of safety is often considered adequate for judging effectiveness of remedial measures. Field monitoring confirmed that the toe-berm did significantly reduce the measured rate of the 731 Block displacements.

A *3DEC* model was used to simulate the excavation of the 731 Block and the placement of the toe-berm. The displacements recorded in the *3DEC* model for the 731 Block exhibited similar trends to that observed in the field and suggests that the toe-berm would be effective in reducing the displacement. The most significant discrepancy with the *3DEC* results is that in the model the largest movements occurred at the toe while in the field the largest movement was recorded at the crest of the slope. This is unresolved and may be due to the lack of undulation/roughness in both the base shear surface and the orientation of the internal discontinuities in the *3DEC* model.

The field records and observations during the failure of the December Slide showed the rock mass exhibited large displacements (approximately 1 m) without catastrophic failure. However, at the end of the movements the rock mass had broken into smaller blocks. This form of progressive failure was simulated by a 'multi-block' model. This model showed that if a slope, such as the 731 Block, was allowed to break into smaller blocks, the ensuing displacements would accelerate and can be large. In addition to the increased resisting force, the placement of the toe-berm after the 731 Block had moved only approximately 100 mm may have been key to the success of the toe-berm in arresting the 731 Block displacements.

Acknowledgements

The authors would like to thank B.C. Hydro for providing access to the necessary data used in this study and for permission to publish this paper.

References

1. Krahn J, R. M. Hardy Address: The limits of limit equilibrium analysis. In: Proceedings 54th Canadian Geotechncial Conference, Calgary, Mahmoud M, van Everdingen R, Carss J, editors, vol. 1, Richmond: BiTech Publishers 2001 pp. 1–18.
2. Holtz R D, Schuster R L, Stabilization of soil slopes. In: Landslides Investigation and Mitigation, Turner A K, Schuster R L, editors, Special Report 247, Washington: National Academy Press 1996 pp. 439–473.
3. Arnao B M, Garga V K, Wright R S, Perez J Y, The Tablachaca Slide No. 5, Peru, and its stabilization. In: The Fourth International Symposium on Landslides, Toronto, vol. 2 1984 pp. 597–604.
4. Fell R, MacGregor J P, Williams J, Searle P, Hue Hue road landslide, Wyong. In: Proceedings Soil Slope Instability and Stabilization, Walker B F, Fell R, editors, Rotterdam: A. A. Balkema 1987 pp. 315–324.
5. Lane L S, Brittle deformation in the Columbia River Fault Zone near Revelstoke, Southeastern British Columbia. Can J Earth Sci 1984, 21:584–598.
6. Moore D P, Imrie A, Rock slope stabilization at Revelstoke Dam. In: Transactions 14th International Congress on Large Dams, Paris, vol. II 1982 pp. 365–385.
7. Small C A, Morgenstern N R, Performance of a highwall in soft rock, Highvale mine, Alberta. Can Geotech J 1992, 29(3):353–363.
8. Martin C D, Kaiser P K, Analysis of a rock slope with internal dilation. Can Geotech J 1984, 21(4):605–620.
9. Sarma S K, Stability analysis of embankments and slopes. ASCE J Geotech Engin Div 1979, 105(GT12):1511–1524.
10. Mostyn G R, Small J C, Methods of stability analysis. In: Proc. Soil slope instability and stabilisation, Sydney, Walker B F, Fell R, editors, Rotterdam: A.A. Balkema 1987 pp. 315–324.
11. Hoek E, General two-dimensional slope stability analysis. In: Analytical and Computational Methods in Engineering Rock Mechanics, Brown E T, editor, London: Allen & Unwin 1987 pp. 95–128.
12. Itasca, Three Dimensional Distinct Element Code: User's Guide. Itasca Consulting Group, Inc, Minneapolis 1999.

13. Starfield A, Cundall PA, Towards a methodology for rock mechanics modeling. Int J Rock Mech Min Sci & Geomech Abstr 1988, 25(3):99–106.
14. Infanti N, Kanji M A, In situ shear strength, normal and shear stiffness determinations at Arua Vermelha project. In: Proceedings Third International Congress of the International Association of Engineering Geologists, Madrid, vol. 2 1978 pp. 175–183.
15. Bishop A W, The use of the slip circle in the stability analysis of slopes. Géotechnique 1955, 5:7–17.
16. Dawson E M, Roth W H, Drescher A, Slope stability analysis by strength reduction. Géotechnique 1999, 49(6):835–840.